



# Biomarker Signatures of Quality for Engineering Nasal Chondrocyte-Derived Cartilage

M. Adelaide Asnaghi<sup>1†</sup>, Laura Power<sup>2†</sup>, Andrea Barbero<sup>1</sup>, Martin Haug<sup>3</sup>, Ruth Köppl<sup>4</sup>, David Wendt<sup>1</sup> and Ivan Martin<sup>1,2\*</sup>

<sup>1</sup> Department of Biomedicine, University Hospital Basel, University of Basel, Basel, Switzerland, <sup>2</sup> Department of Biomedical Engineering, University of Basel, Basel, Switzerland, <sup>3</sup> Department of Surgery, University Hospital Basel, Basel, Switzerland, <sup>4</sup> Otorhinolaryngology, Head and Neck Surgery, University Hospital Basel, Basel, Switzerland

## OPEN ACCESS

### Edited by:

Martijn van Griensven,  
Maastricht University, Netherlands

### Reviewed by:

Gerjo Van Osch,  
Erasmus Medical Center, Netherlands  
Niamh Fahy,  
Erasmus University Rotterdam,  
Netherlands

### \*Correspondence:

Ivan Martin  
ivan.martin@usb.ch

† These authors have contributed  
equally to this work

### Specialty section:

This article was submitted to  
Tissue Engineering and Regenerative  
Medicine,  
a section of the journal  
Frontiers in Bioengineering and  
Biotechnology

**Received:** 17 January 2020

**Accepted:** 18 March 2020

**Published:** 07 April 2020

### Citation:

Asnaghi MA, Power L, Barbero A,  
Haug M, Köppl R, Wendt D and  
Martin I (2020) Biomarker Signatures  
of Quality for Engineering Nasal  
Chondrocyte-Derived Cartilage.  
*Front. Bioeng. Biotechnol.* 8:283.  
doi: 10.3389/fbioe.2020.00283

The definition of quality controls for cell therapy and engineered product manufacturing processes is critical for safe, effective, and standardized clinical implementation. Using the example context of cartilage grafts engineered from autologous nasal chondrocytes, currently used for articular cartilage repair in a phase II clinical trial, we outlined how gene expression patterns and generalized linear models can be introduced to define molecular signatures of identity, purity, and potency. We first verified that cells from the biopsied nasal cartilage can be contaminated by cells from a neighboring tissue, namely perichondrial cells, and discovered that they cannot deposit cartilaginous matrix. Differential analysis of gene expression enabled the definition of identity markers for the two cell populations, which were predictive of purity in mixed cultures. Specific patterns of expression of the same genes were significantly correlated with cell potency, defined as the capacity to generate tissues with histological and biochemical features of hyaline cartilage. The outlined approach can now be considered for implementation in a good manufacturing practice setting, and offers a paradigm for other regenerative cellular therapies.

**Keywords:** regenerative medicine, engineered cartilage, perichondrium, identity/purity, potency, quality controls, advanced therapy medicinal product, good manufacturing practice

## INTRODUCTION

Large cartilage defects in adults have limited capacity to regenerate, and state-of-the-art regenerative medicine therapies do not induce reproducible or stable results (Kon et al., 2009; Teo et al., 2019). We previously demonstrated the safety and feasibility of autologous nasal chondrocyte-derived engineered cartilage for the treatment of focal traumatic lesions in the knee in a phase I clinical trial (Mumme et al., 2016), and a phase II clinical trial is ongoing to investigate efficacy. Briefly, autologous nasal chondrocytes are expanded *in vitro* before seeding onto a collagen I/III scaffold and cultured in chondrogenic conditions to produce a mature, hyaline-like cartilage graft that is then implanted into the knee cartilage defect of the same patient.

The starting material for this approach is a biopsy from the native nasal septum cartilage, which, like articular cartilage, is a hyaline cartilage (Al Dayeh and Herring, 2014) composed predominantly of water, type II collagen, glycosaminoglycan (GAG) containing proteoglycans, and the one cell type, chondrocytes (Buckwalter and Mankin, 1998). Mucoperichondrium is the tissue that overlays nasal cartilage; it consists of several layers, including mucosa, lamina propria, and perichondrium, the tissue directly adjacent to the cartilage that is tightly attached and cannot be easily distinguished

(Aksoy et al., 2012). Currently, nasal septal cartilage and mucoperichondrium are separated by pulling them apart with forceps and are identified based on their physical characteristics. Due to donor-related and operator-related variability, the resulting biopsy may not be completely pure after cleaning, with some overlaying tissue remaining attached to the cartilage.

When working with intrinsically variable donor-derived human materials, such as tissues and cells, establishing the quality and consistency of the starting material is key to ensuring reproducibly high quality engineered products, not least to avoid the consequences of cell misidentification (Editorial, 2009; Hyun-woo, 2019). This prompts for the development of identity and purity assays (Carmen et al., 2012), which can be based on various characteristics of the cells, such as gene or protein expression. Gene expression markers have been proposed for articular cartilage cell identity and purity assays (Mollenhauer and Gaissmaier, 2010; Bravery et al., 2013; Committee for Medicinal Products for Human Use [CHMP], 2017; Diaz-Romero et al., 2017). However, until now, there are no known biomarkers that can distinguish the cell types found in nasal cartilage biopsies. Moreover, the impact of possibly contaminating cells on nasal chondrocyte-based engineered cartilage has not been investigated.

Engineered products treat diseases or damage through repairing, replacing, or regenerating tissues or organs (Detela and Lodge, 2019). A potency assay must be developed based on the mode of action of the tissue engineered product (Committee for Medicinal Products for Human Use [CHMP], 2008)—in our case, the filling of cartilage defects with healthy, hyaline-like tissue—which is ideally correlated to the efficacy, leading to consistent quality of the tissue engineered product and good clinical outcome (Bravery et al., 2013). Gene expression markers have been investigated for human articular chondrocytes (Dell'Accio et al., 2001; Rapko et al., 2010), but not for cells from the nasal septum.

In this study, we first investigate which cell types are potentially contaminating in human nasal septum cartilage biopsies and their impact on the quality of engineered cartilage. We then investigated whether gene expression analysis could discriminate the contaminant cells found in nasal septal biopsies for the development of a characterization panel for identity and purity quality controls. To assess potency, we compared the gene expression of nasal septum biopsy-derived cells to their ability to produce cartilaginous tissue. Finally, we propose how these purity and potency assays could be implemented in a good manufacturing practice (GMP) compliant process for the translation of our regenerative therapy product.

## MATERIALS AND METHODS

### Cell Isolation and Expansion

Human nasal septum biopsies were collected from 17 donors (9 female, 8 male, mean age 46 years, range 16–84 years) undergoing reconstructive surgery after informed consent and in accordance with the local ethical commission (EKBB; Ref.# 78/07). Two samples derived from patients enrolled in the Nose2Knee

clinical trials (ClinicalTrials.gov, number NCT01605201 and number NCT02673905).

For four donors, the biopsy was dissected to give a pure nasal cartilage sample (NC) and a pure perichondrium sample (PC).

Nasal chondrocytes were isolated from NC by enzymatic digestion as previously described (Jakob et al., 2003) with 0.15% collagenase II (Worthington) for 22 h at 37°C. After digestion, NCs were plated in tissue culture flasks at a density of  $1 \times 10^4$  cells/cm<sup>2</sup> and cultured in medium consisting of *complete medium* [Dulbecco's Modified Eagle's Medium (DMEM)] containing 4.5 mg/mL D-glucose and 0.1 mM non-essential amino acids, 10% fetal bovine serum (FBS), 1 mM sodium pyruvate, 100 mM HEPES buffer, 100 U/mL penicillin, 100 µg/mL streptomycin, and 0.29 mg/mL L-glutamine (all from Invitrogen). Complete medium was supplemented with 1 ng/mL transforming growth factor beta-1 (TGF-β1) and 5 ng/mL fibroblast growth factor-2 (FGF-2) (both from R&D Systems) at 37°C and 5% CO<sub>2</sub> in a humidified incubator (Thermo Scientific Heraeus) as previously described (Jakob et al., 2003). When approaching 80% confluence, cells were detached using 0.05% trypsin-EDTA (Invitrogen) and re-plated.

Perichondrium tissue samples were cut in small pieces and put on the bottom of plastic culture dishes to isolate adherent cells that migrated out of the tissue for 1 week in complete medium. Cells were then detached using 0.05% trypsin-EDTA and further cultured until confluence in the same conditions as nasal chondrocytes.

Specific ratios of NC to PC cells were combined at passage two to generate mixed populations of *known* purity of 100, 90, 80, 70, 60, and 0% NC.

For all other biopsies, in case perichondrium was present, half was dissected, removing all perichondrium to obtain a NC, while the overlaying perichondrium remained intact on the other half (labeled as NC + PC samples, containing variable numbers of NC and PC cells). Cells were isolated from each sample by enzymatic digestion and expanded in complete medium supplemented with TGF-β1 and FGF-2 up to two passages as described above for nasal chondrocytes.

### Proliferation Rate

Proliferation rates were calculated as the ratio of  $\log_2(N/N_0)$  to T, where  $N_0$  and N are the numbers of cells respectively at the beginning and at the end of the expansion phase,  $\log_2(N/N_0)$  is the number of cell doublings, and T is the time required for the expansion.

### Chondrogenic Redifferentiation Micromass Pellets

Cells expanded until passage two were redifferentiated by culturing as 3D micromass pellets, as previously described (Asnaghi et al., 2018). 3D micromass pellets were formed by centrifuging  $5 \times 10^5$  cells at  $300 \times g$  in 1.5 mL conical tubes (Sarstedt) and cultured for 2 weeks in chondrogenic serum-free medium consisting of DMEM containing 1 mM sodium pyruvate, 100 mM HEPES buffer, 100 U/mL penicillin, 100 µg/mL streptomycin, 0.29 g/mL L-glutamine, 1.25 mg/mL human serum albumin (CSL Behring), and 100 nM

dexamethasone (Sigma, Switzerland), supplemented with 10 ng/mL TGF- $\beta$ 1 (R&D), ITS + 1 (10  $\mu$ g/mL insulin, 5.5  $\mu$ g/mL transferrin, 5 ng/mL selenium; Gibco), 100  $\mu$ M ascorbic acid 2-phosphate (Sigma), and 4.7  $\mu$ g/mL linoleic acid (Sigma). Culture medium was changed twice weekly.

### Engineered Cartilage on Chondro-Gide

Passage two cells were seeded on collagen type I/III membranes (Chondro-Gide; Geistlich Pharma AG) at a density of 4.17 million cells per cm<sup>2</sup>. The resulting constructs were cultured for 2 weeks in chondrogenic medium consisting of complete medium supplemented with 10  $\mu$ g/mL insulin (Novo Nordisk), and 0.1 mM ascorbic acid 2-phosphate (Sigma) at 37°C and 5% CO<sub>2</sub> with media changes twice/week.

The described protocols match the ones used in the context of the clinical trial, where GMP-grade reagents and autologous serum instead of FBS are used. Grafts for clinical use are produced at the GMP facility at the University Hospital Basel according to standard operating procedures under a quality management system, as described in Mumme et al. (2016).

### Histology and Immunohistochemistry

Samples were fixed overnight in 4% formalin and embedded in paraffin. Sections 5  $\mu$ m in thickness were stained with safranin O for GAGs and hematoxylin as a nuclear counterstaining as described elsewhere (Grogan et al., 2006). Immunohistochemistry against collagen type I (No. 0863170, MP Biomedicals, 1:5000) and collagen type II (No. 0863171, MP Biomedicals, 1:1000) was performed using the Vectastain ABC Kit (Vector Labs) with hematoxylin counterstaining as in standard protocols (Scotti et al., 2010). Incubation of tissues with only the secondary antibody were used as negative controls.

Histological scoring via the modified Bern score (MBS) was performed on safranin O-stained histological images as previously described (Lehoczky et al., 2019), as adapted from Grogan et al. (2006). Briefly, the MBS has two rating parameters that each receive a score between 0 and 3. First, the intensity of safranin-O staining (0 = no stain; 1 = weak staining; 2 = moderately even staining; 3 = even dark stain), and second, the morphology of the cells (0 = condensed/necrotic/pycnotic bodies; 1 = spindle/fibrous; 2 = mixed spindle/fibrous with rounded chondrogenic morphology; 3 = majority rounded/chondrogenic). The two values are summed together resulting in a maximum possible MBS of 6.

### qPCR

We chose the gene expression markers to investigate based on a literature search. Interested in both purity and potency assays, we focused on matrix associated genes considering the two cell types potentially present in our starting material derive from tissues with structurally different ECM. The gene expression ratios of collagen II to I and aggrecan to versican are well-known chondrogenic markers (Martin et al., 2001). HAPLN1 has been found in most types of cartilage (Spicer et al., 2003), including in bovine nasal cartilage (Baker and Caterson, 1978). Versican protein expression has been found in perichondrium from other cartilage tissue sources (Shibata et al., 2001) and nestin

has been shown to be expressed in embryonic perichondrium (Ono et al., 2014). MFAP5 is found in elastic as well as non-elastic extracellular matrixes (Halper and Kjaer, 2014) and has been used as a negative marker for chondrogenic cells from articular cartilage (Rapko et al., 2010).

Total RNA was extracted from expanded cells at both P1 and P2, 3D micromass pellets, and engineered cartilage grafts with the Quick RNA Miniprep Plus Kit (Zymo Research) and quantitative gene expression analysis was performed as previously described (Martin et al., 2001). Reverse transcription into cDNA was done from 3  $\mu$ g of RNA by using 500  $\mu$ g/mL random hexamers (Promega, Switzerland) and 0.5  $\mu$ L of 200 UI/mL SuperScript III reverse transcriptase (Invitrogen). Assay on demand was used with TaqMan Gene Expression Master Mix to amplify type I collagen (Col I, Hs00164004), type II collagen (Col II, Hs00264051), aggrecan (Agg, Hs00153936\_m1), Versican (Ver, Hs00171642\_m1), link protein 1 (HAPLN1, Hs00157103\_m1), MFAP5 (MFAP5, Hs00185803\_m1), nestin (Nes, Hs00707120\_s1), and GAPDH (GAPDH, Hs00233992\_m1) (all from Applied Biosystems). The threshold cycle (C<sub>T</sub>) value of the reference gene, GAPDH, was subtracted from the C<sub>T</sub> value of the gene of interest to derive  $\Delta$ C<sub>T</sub> values. All displayed gene expression levels are, and statistical analyses were performed on, the  $\Delta$ C<sub>T</sub> values. GAPDH was found to be a stable reference gene for both nasal chondrocytes and perichondrial cells with a mean  $\Delta$ C<sub>T</sub> value of 18.1 (standard deviation of 0.68) at passage 2 and 22.6 (standard deviation of 0.80) for pelleted cells across both cell types.

### Biochemical Quantification of GAG and DNA

Samples of engineered cartilage and micromass pellets were digested with proteinase K (1 mg/mL proteinase K in 50 mM Tris with 1 mM EDTA, 1 mM iodoacetamide, and 10 mg/mL pepstatin A) for 16 h at 56°C. The GAG content was determined as previously described (Barbosa et al., 2003). Briefly, samples were incubated with 1 mL of dimethylmethylene blue assay (DMMB; Sigma-Aldrich 341088) solution (16 mg/L dimethylmethylene blue, 6 mM sodium formate, 200 mM GuHCL, pH 3.0) on a shaker at room temperature for 30 min. Precipitated DMMB-GAG complexes were centrifuged and supernatants were discarded. Complexes were dissolved in decomplexion solution (4 M GuHCL, 50 mM Na-acetate, 10% propan-1-ol, pH 6.8) at 60°C, absorption was measured at 656 nm and GAG concentrations were calculated using a standard curve prepared with purified bovine chondroitin sulfate. DNA content was measured using the CyQuant Cell Proliferation Assay Kit (Invitrogen) according to the instructions of the manufacturer.

### Modeling

The generalized linear modeling (glm) function in R was used to build all the models. A logistic regression model was used to predict purity, where the response is a continuous probability between 0 (pure perichondrium) and 1 (pure cartilage) with samples from four donors and 48 independent experiments of known purities. For the logistic regression models, the

McFadden pseudo  $R^2$  values were calculated with the `pscl` R package (Jackman, 2017) and the Hosmer–Lemeshow analysis was performed with the `ResourceSelection` R package (Lele et al., 2019). For the potency assay predicting GAG production, a gamma GLM with a log link was used to model quantified amounts of GAG (measured in  $\mu\text{g}$ ). The MBS of chondrogenic pellets was modeled by first dividing the value by six, the maximum possible score, then training a multiple logistic regression model; the predicted responses were then multiplied by six. Samples from nine donors in 28 independent experiments were used to train the MBS potency assay and 25 independent experiments were used to train the GAG potency model and for gene selection. For all three assays, stepwise selection (Agostini et al., 2015) was performed in both directions; collagen II and I, aggrecan, versican, HAPLN1, and MFAP5 were tested and the model with the lowest Akaike information criterion (AIC) was chosen. Samples from five donors in 12 independent experiments were used to test the potency models. Residual plots were used to verify all the models. The correlation between the predicted and actual purity, GAG, and MBS values were calculated with the square of the Pearson correlation coefficient. The final equations of the potency models were rebuilt with both the training and test data together.

## Statistical Analysis

All calculations were performed using standard functions, unless otherwise stated, in R (R Core Team, 2019). Statistical significance is defined as  $p < 0.05$ . Statistical significance for comparing two means was calculated using paired or unpaired  $t$ -tests and normality was checked with the Shapiro–Wilk test. To test multiple comparisons, a linear model was fitted, then the `glht` function of the `multcomp` R package (Hothorn et al., 2008) was used to test all the contrasts;  $p$ -values were corrected for multiple testing using the single-step Bonferroni method. Correlation plots using Spearman correlation coefficients ( $\rho$ ) were created with the `corrplot` R package (Wei and Simko, 2017). Data are presented as mean and standard deviation of independent experiments with cells from at least 4 different donors. For each analysis at least 2 replicate micromass pellets were used per condition. Symbols used are: \*\*\* $p < 0.001$ , \*\* $p < 0.01$ , \* $p < 0.05$ , and  $p < 0.1$ .

## RESULTS

### Native Nasal Septum Biopsy Characterization

In the context of ongoing clinical trials, the nasal septum biopsy is harvested along the subperichondrial axis, so that most of the perichondrium remains in place in the patient's nose, not only an efficient risk-control measure, but also important for the stability and healing of the donor site. More heterogeneous samples are obtained from plastic surgeries unrelated to clinical trials, which include mixed cartilage and perichondrium. Safranin O staining of nasal septum specimens indicated the presence of tissues with distinct characteristics, i.e., GAG-rich cartilage with

round chondrocytes residing in lacunae and adjacent GAG-negative perichondrium containing cells with fibroblast-like morphology, comparable to previous findings (Bairati et al., 1996). Immunohistochemical analysis showed more collagen II in the cartilage and more collagen I in the perichondrium, confirming previously reported results (Popko et al., 2007). The border between the two tissues is not clearly defined in our samples, as in previous reports (Bairati et al., 1996; **Figure 1A**).

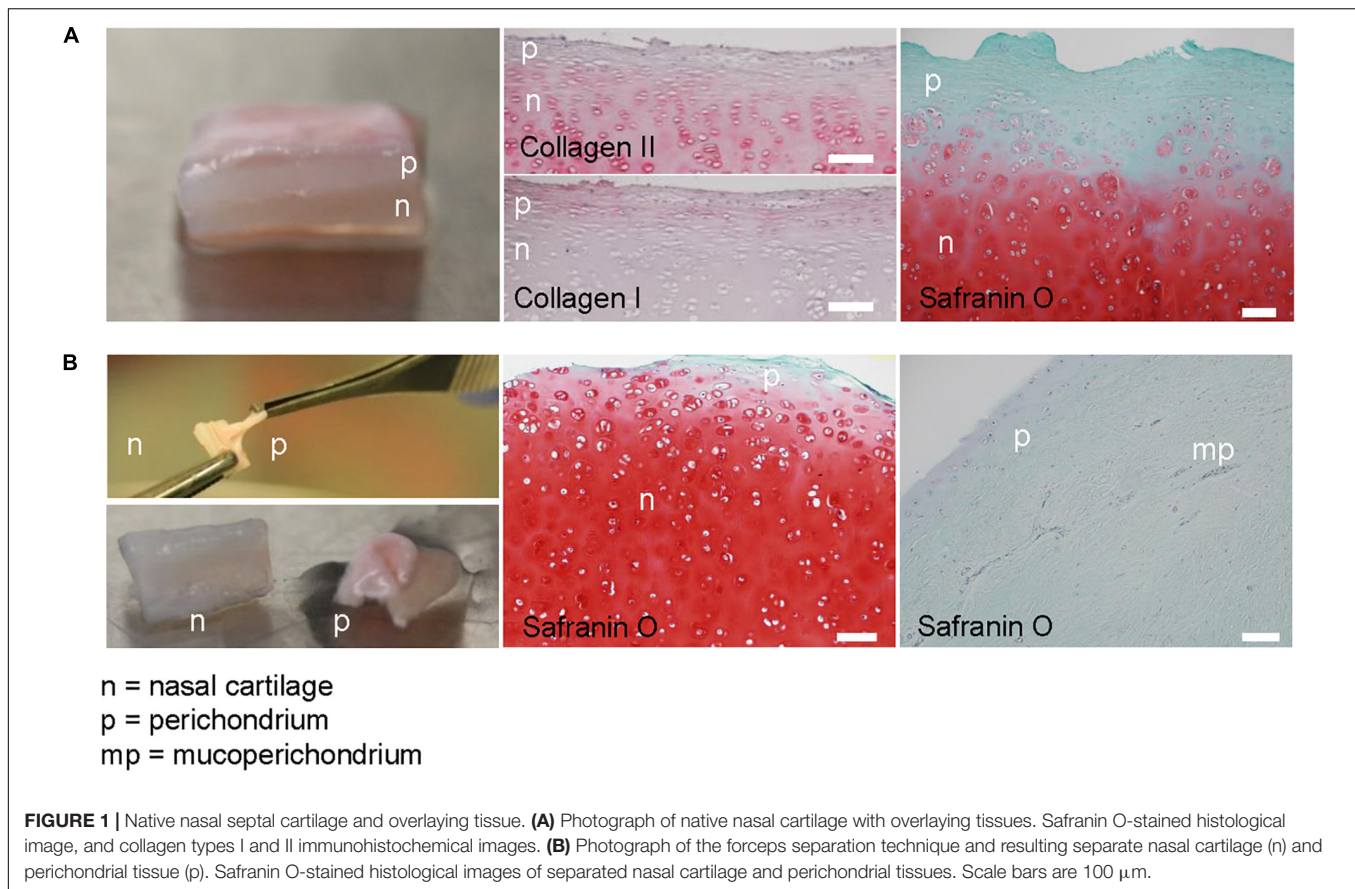
The separation of the cartilage and overlaying tissue is done by pulling them apart with forceps; however, the efficiency of this technique is unknown. Histological analysis after physical separation of cartilage and perichondrium revealed that the resulting biopsy may have small amounts of safranin O-negative tissue on the cartilage after separation (**Figure 1B**). This safranin O-negative region includes cambium, which is hypothesized to be the source of cells with tissue forming capacity (Upton and Glowacki, 1981; Van Osch et al., 2000), and sometimes perichondrium that is difficult to remove (Hellingman et al., 2011). Deeper cleaning of the starting biopsy (e.g., via scraping or cutting with a scalpel) is not a suitable option, since we observed reduced cell yield and slightly lower chondrogenic capacity in preliminary experiments, supporting the theory that this superficial region contains more potent cells.

### Characterization of Perichondrial Cells

The samples we classify as NC and PC are the tissues after separation using the aforementioned technique. Visually, under macroscopic observation during expansion in cell culture dishes, NC and PC cells are not distinguishable, both having the same characteristic fibroblastic-like cell morphology. The proliferation rates of the two cell types were measured and found to be about equal (**Figure 2A**). To compare the chondrogenic capacity of NC and PC cells, we engineered pellets and found that NCs could reproducibly produce GAG and collagen II while PCs could not and predominantly produced type I collagen, as seen by histological analyses and biochemical quantification (**Figures 2B,C**).

### Identity Assay

We sought to distinguish the cells from these two tissues based on their gene expression profiles. NC cells expressed significantly higher levels of type II collagen and relative ratios of collagen II:I, aggrecan:versican and, at passage two, HAPLN1:MFAP5; whereas PC cells expressed significantly higher levels of versican, MFAP5, and nestin (**Figure 3**). Expanded cells were then cultured as 3D micromass pellets in chondrogenic conditions for two more weeks. NC cells from engineered pellets expressed significantly more collagen II and higher ratios of collagen II:I, aggrecan:versican, and HAPLN1:MFAP5, and PC cells expressed significantly higher levels of versican and MFAP5 (**Supplementary Figure S1**). In summary, these results demonstrate that nasal chondrocytes and perichondrial cells have statistically significant differential expression of cartilage-related genes both during expansion and after pellet culture.



## Purity Assay

The only method currently available to assess the purity of the starting native cartilage biopsy is by manually counting the number of cells in each type of tissue in a histological image (**Supplementary Figure S2**). This method suffers from limitations due to histological artifacts, unclear distinction between tissue types, its semi-quantitative and destructive nature, and the fact that a histological section may not be representative of the whole tissue. Here we assessed if the purity of a *mixed* cell population could also be estimated based on gene expression analysis.

Spearman correlation coefficients ( $\rho$ ) of the gene expression of cells at passage two that we combined at specific ratios of NC and PC cells revealed statistically significant trends across donors. Due to high donor-to-donor variability, the correlations between cell population purity and gene expression were higher per donor per gene than across donors. The highest correlation was found for the relative expression of aggrecan:versican ( $\rho = 0.69$ ), where the ratio was higher in purer populations containing more NCs; per donor the correlations were even stronger ( $\rho = 0.61\text{--}0.98$ ) (**Supplementary Figure S3A**).

In general, more significant differences in gene expression in individual genes and cell purity were seen at passage two compared to the pelleted cells' gene expression (**Supplementary Figure S3B**). Therefore, we focused on passage two for the subsequent purity model.

We performed multiple logistic regression to compare gene expression of collagen type I and II, aggrecan, versican, MFAP5, HAPL1, and nestin to the cell population purity. To gain insight into which genes were most important, stepwise selection (Agostini et al., 2015) was implemented and the model with the lowest AIC was chosen. Versican and collagen type II were found to be the factors most predictive of purity and significantly contributed to the model ( $p\text{-value} = 2.7\text{e-}3$ ,  $p = 2.8\text{e-}3$ , respectively, and overall, the model was significant (Hosmer–Lemeshow  $p = 0.95$  and McFadden pseudo  $R^2 = 0.53$ ). The coefficient estimates from the model and the  $\Delta\text{Ct}$  values for versican and collagen II can be used to estimate the purity of a population of nasal cartilage-derived cells using Eq. 1, where inverse logit is  $\exp(x) / [1 + \exp(x)]$ .

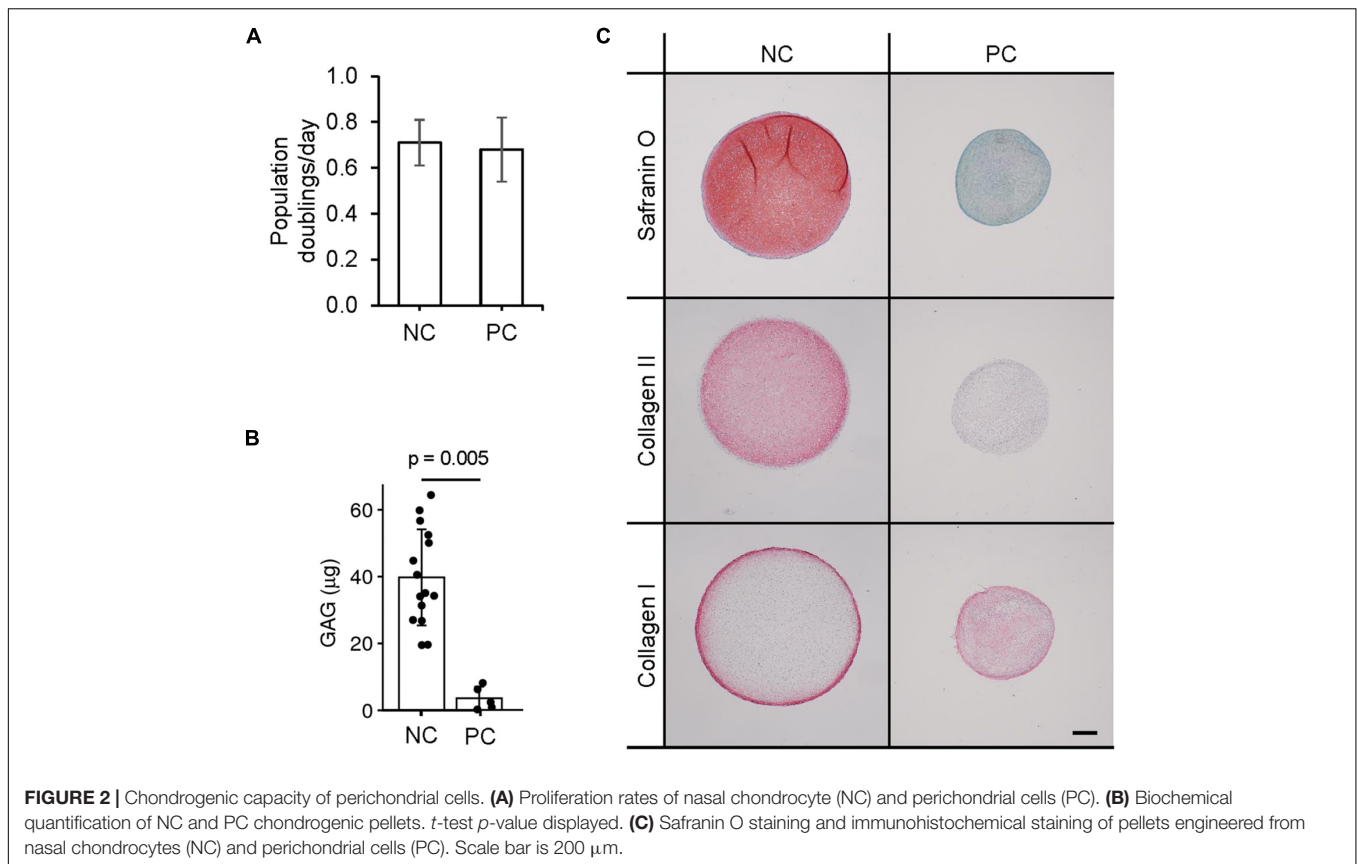
Purity (NC%)

$$= \text{inverse logit} [1.93 + (\text{Col2}) \times 0.64 - (\text{Ver}) \times 1.08] \quad (1)$$

The purity predicted by the model was plotted against the known purity and the resulting  $R^2$  value of the observed and predicted values was 0.79 (**Figure 4**).

## Potency Assay

We investigated whether predictive gene expression markers can be used to estimate the capacity of the cells to form engineered



cartilage. The final cartilage quality is currently assessed using the MBS, a semi-quantitative score of safranin O-stained histological images (Grogan et al., 2006; Lehoczy et al., 2019), and via GAG quantification (Thej and Kumar Gupta, 2019).

GAG content as well as the histological MBS score of the chondrogenic pellets were positively correlated to the cartilage identity gene expression markers and negatively correlated to the perichondrial identity markers (**Supplementary Figure S4**). The interrelationship of potency and purity is visualized in the top left corner of the correlation plot, which shows that purity (NC%), GAG, GAG/DNA, and MBS are highly correlated (**Figure 5**).

More significant gene expression trends were seen when analyzing the cells at passage two compared to after engineered pellet culture, so we developed a potency assay for this time point.

In order to develop a potency assay that could predict the amount of GAG in the final engineered cartilage based on the gene expression of the starting cell population, we trained a generalized linear model with a log-link and gamma distribution. The gamma distribution was selected because it only predicts positive values and because its distribution is flexible enough to fit many response shapes (Hardin and Hilbe, 2007). To select which gene expressions could best predict GAG produced by cells culture as pellets, stepwise selection was performed. Collagen II and MFAP5 were found to be the most significant and the model showed good results (training  $R^2 = 0.34$  and testing  $R^2 = 0.78$  of observed vs. predicted values; **Figure 6A**). The equation of the potency assay to predict the amount of GAG produced via the

gene expression of passage two cells (Eq. 2), where the  $\Delta$ Ct values of the genes should be entered, was generated using both the test and training data together, to report the most accurate coefficient estimates possible.

Potency [GAG ( $\mu$ g)]

$$= \exp [2.55 + (\text{Col2}) \times 0.06 - (\text{MFAP5}) \times 0.14] \quad (2)$$

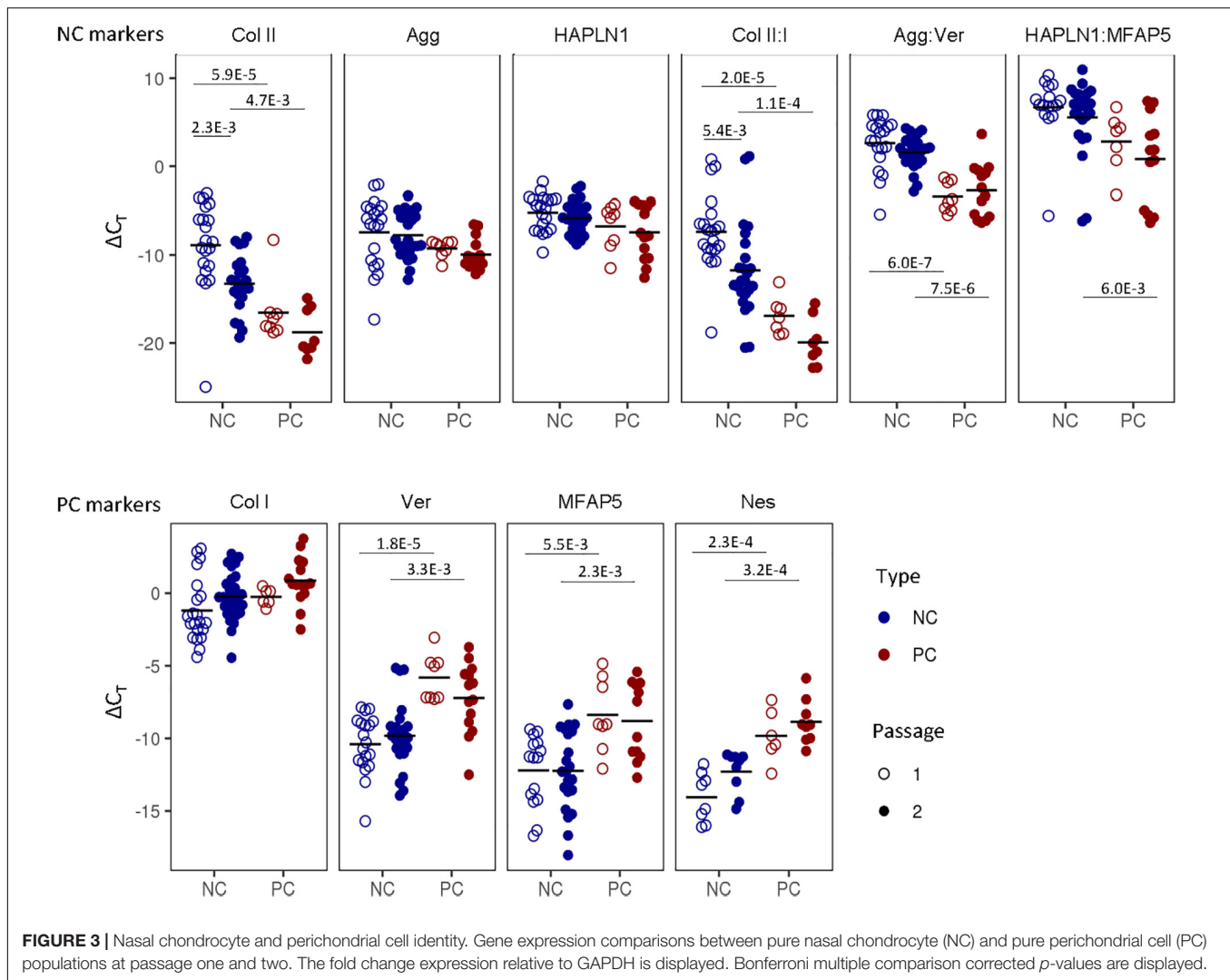
For a potency assay that can predict the histological score of the final engineered cartilage from passage two gene expression, a logistic regression model was trained. Stepwise selection found that the best model included only the MFAP5 gene, and showed good predictive ability in this dataset (training  $R^2 = 0.54$  and testing  $R^2 = 0.64$  of observed vs. predicted values; **Figure 6B**). The equation of the potency assay to predict the histological MBS score (Eq. 3), where the  $\Delta$ Ct value of the gene should be used, was generated with both the training and test data together. Again, the inverse logit is  $\exp(x) / [1 + \exp(x)]$ , imposing upper and lower bounds on the model.

Potency (histological score, MBS) (3)

$$= 6 \times \text{inverse logit} [-0.84 - (\text{MFAP5}) \times 0.21] \quad (4)$$

## Implementation of In-Process Controls

Since isolated nasal septum-derived cell populations may include some perichondrial cells, we tested the impact of various amounts



of contaminating cells on final engineered cartilage quality. The chondrogenic capacity of contaminated cell populations was consistently lower than of pure cell populations, as observed across 15 donors, demonstrated by safranin O staining, GAG quantification, and immunohistochemical analysis of collagen types II and I (**Supplementary Figure S5**). We confirmed the negative effect of perichondrial cells on the engineered cartilage not only in pellet culture, but also when produced according to the clinical trial protocol where cells are seeded onto a collagen I/III scaffold (**Supplementary Figure S6**).

A threshold of acceptable purity needs to be set to guarantee the quality of the final product. Known quantities of NC and PC cells were mixed together and chondrogenic pellets were produced. Histological scoring was then used to set acceptable limits of PC cell contamination so that the quality of the final product would still meet the clinical trial release criteria ( $MBS \geq 3$ ). Due to donor-to-donor variability, potential cross-contamination from the mechanical tissue separation method, and considering the limitations of histological analysis, we show that some donors could still produce cartilage matrix of sufficient

quality with up to 40% PC contamination, while the less potent donors could produce cartilage matrix with a PC contamination of up to 30% PC cells (**Figure 7A**).

Using the purity and potency assays we developed, the quality was estimated based on the gene expression of passage two cell populations for clinical trial samples and for heterogeneous biopsies collected from patients that underwent plastic surgeries with variable amounts of overlying perichondrium. The predicted histological score results closely matched the actual values, and the quantified amounts of GAG could be estimated well, predicting if cells would produce high or low amounts of GAG (**Figure 7B**). The clinical trial starting materials were assessed to be pure. The potency assay predicted good chondrogenic capacity, confirmed by the high quality of the engineered cartilage produced in the clinical trial. The quality of the grafts also correlated to a good clinical outcome at the 24-month follow up examination, as demonstrated by a significant increase in KOOS scoring, where patients report their symptoms, pain levels, knee function, ability to do sport, and quality of life (Mumme et al., 2016). The more heterogeneous

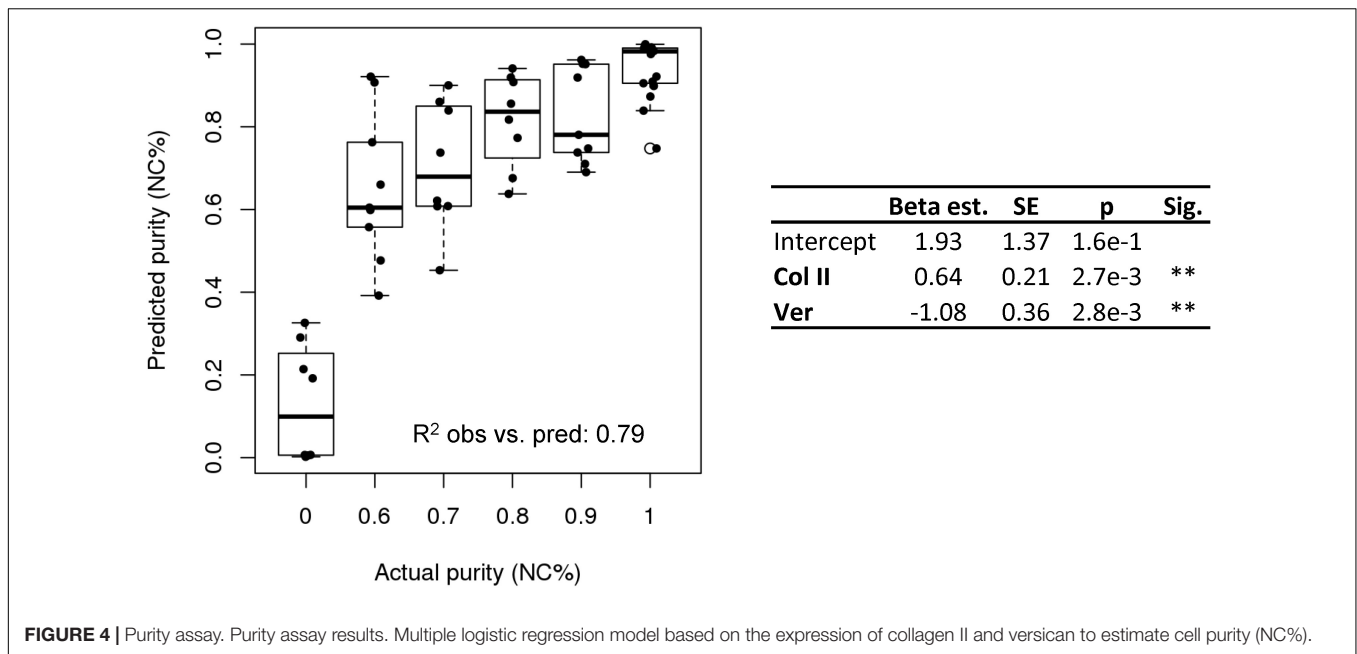


**FIGURE 4 |** Purity assay. Purity assay results. Multiple logistic regression model based on the expression of collagen II and versican to estimate cell purity (NC%).

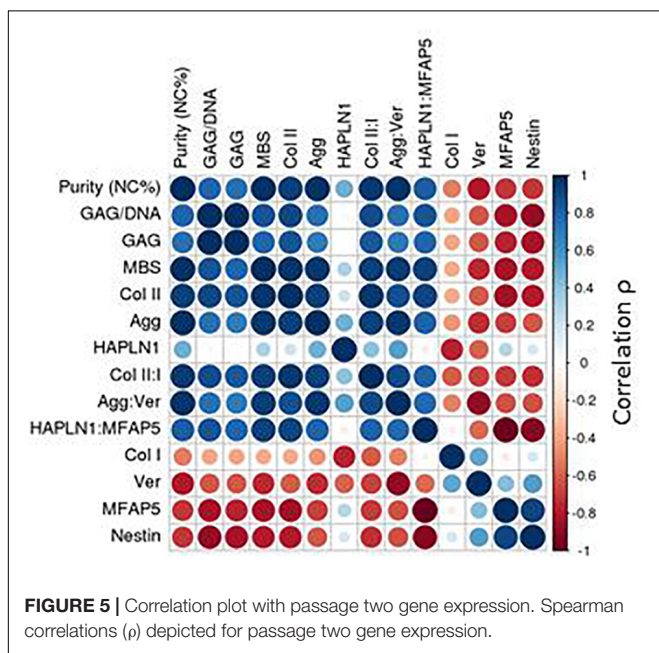


**FIGURE 5 |** Correlation plot with passage two gene expression. Spearman correlations ( $\rho$ ) depicted for passage two gene expression.

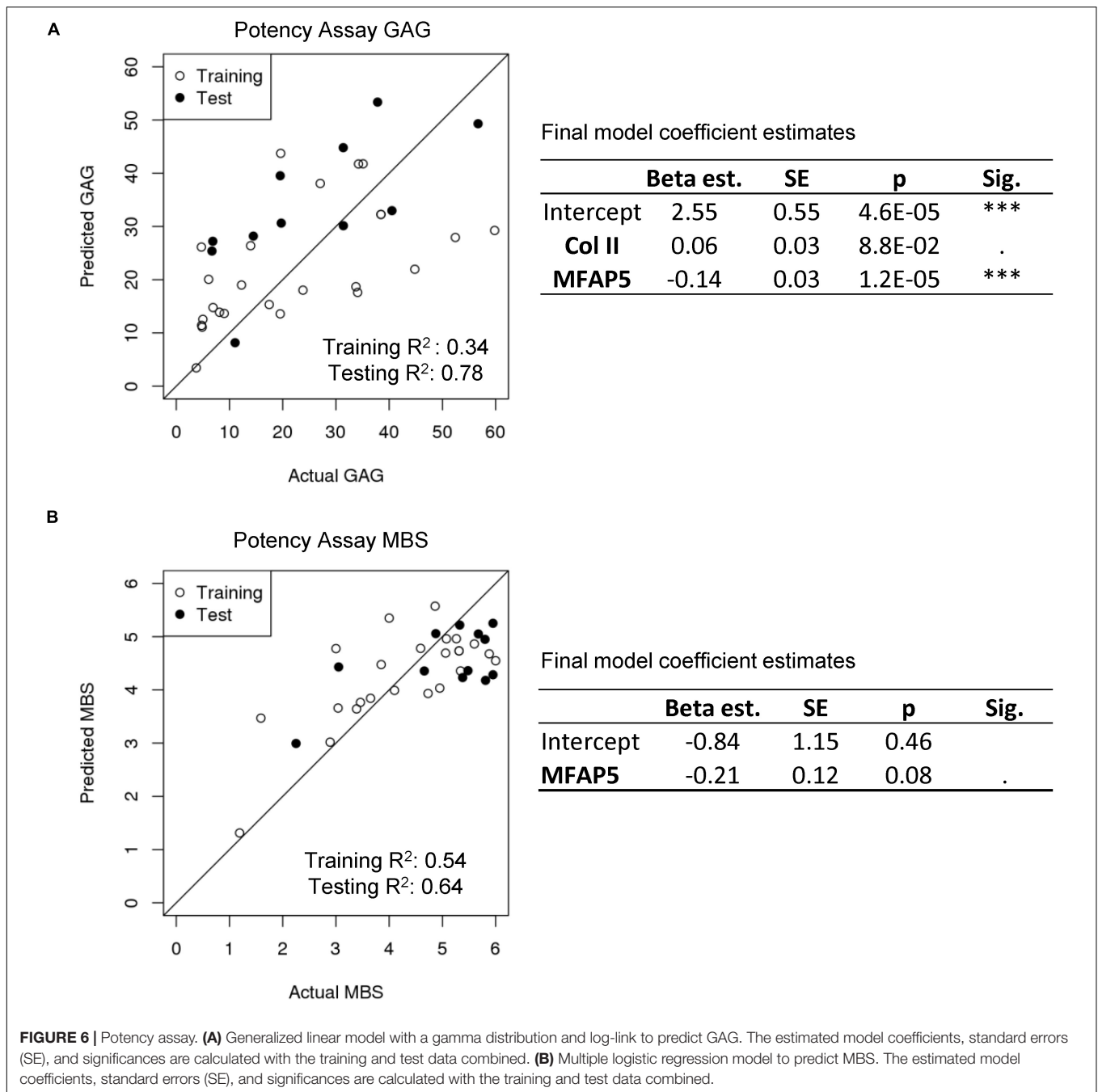
## DISCUSSION

In this study, we established novel in-process controls to ensure the quality and standardization of nasal chondrocyte-based engineered cartilage grafts. Histological analysis revealed that nasal septal cartilage may be harvested with some adjacent tissue, and that there may still be fragments of perichondrial tissue overlaying the cartilage even after a trained operator further separates the tissues. Although some researchers claim that perichondrial cells from other cartilage sources have chondrogenic potential (Hellingman et al., 2011), we discovered that unlike chondrocytes, nasal septal perichondrial cells do not have the capacity to form GAG- and collagen type II-rich engineered tissues. We found that increasing amounts of perichondrium in the starting material profoundly decreases the quality of engineered cartilage, as seen by less GAG and collagen II production during chondrogenic culture. Therefore, minimal contamination of perichondrial cells must be ensured. The NC identity marker we found is collagen II, and the PC identity markers were, versican, MFAP5, and nestin. To quantitatively determine the percentage of contaminating cells in a population, we developed a model that correlates the expression of multiple gene expression markers to the purity of a cell population. Similarly, to predict the chondrogenic capacity of a cell population, we built models to estimate GAG production and the final histological MBS score in engineered cartilage. Finally, we discuss how such quality controls could be implemented during the production of cell or tissue therapies.

In practice, quantitative reverse-transcription polymerase chain reaction (qPCR) instrumentation is ubiquitous, so a gene expression-based quality control could be easily implemented. The cost of the quality control assay could be reduced by selecting a handful of genes for a standard qPCR analysis compared to transcriptomic analysis or single-cell RNA sequencing, and for a

cartilage samples from plastic surgery procedures had more variable results. The purity assay predicted the worst sample to have a purity of 20%, many samples to be 99% pure, and the mean purity of mixed samples to be 75% (Figure 7C). Consistent with the established purity threshold, cells that were predicted to be >70% pure were all able to produce cartilaginous tissues that passed the histological score release criteria. The sample with a predicted purity of 20%, on the other hand, produced a pellet that failed the release criteria (histological score = 2.3).

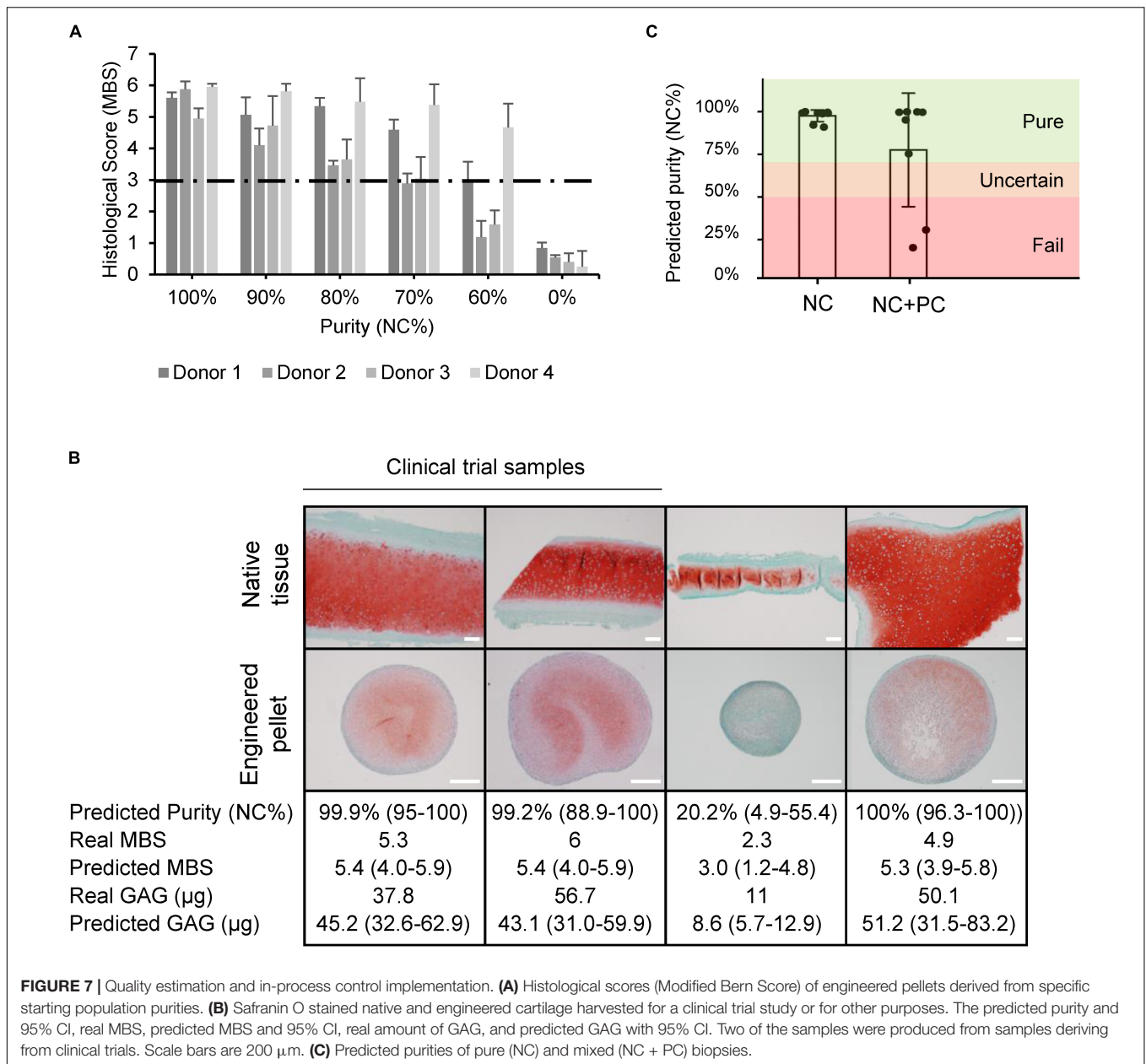




routine test could be enough information to confirm cell identity (Maertzdorf et al., 2016).

To implement such gene expression-based quality controls, a suitable time point during the manufacturing process must be chosen. Biomarkers vary not only spatially within the tissue, but also temporally during monolayer expansion and after tissues are engineered (Tay et al., 2004; Späth et al., 2018; Detela and Lodge, 2019), and it also may be that the cells have more distinct gene expression profiles at certain time points than others (Tekari et al., 2014). From a practical perspective, an earlier quality control would save costs, because the quality of

the cells could be established before an expensive production is undertaken. However, after 1 or 2 weeks of cell expansion, there are many more cells and an aliquot can be taken without depleting the whole cell population and the gene expression analysis of an aliquot of a cell suspension provides a broad readout of the total cellular material. Obtaining cells before they are embedded in the scaffold would allow to perform the analysis non-destructively. Interestingly, despite passage two corresponds to variable numbers of population doublings and thus to different degrees of cell de-differentiation, the biomarkers we investigated had the most distinct expression levels after the expansion phase.



Consequently, we propose that our gene expression-based assays should be implemented on expanded passage two cells.

Generalized linear models for the development of gene expression-based quality controls for regenerative medicine is a natural extension of their use in biomarker-based disease diagnosis (Faraway, 2006; Hosmer et al., 2013). Here we show how multiple logistic regression can be used to model purity percentages with the advantage of being able to provide biologically relevant estimates, i.e., between 0 and 100% (Zhao et al., 2001). When further screening the most significant genes that contributed to the purity model with stepwise selection (Ying et al., 2018; Liu et al., 2019), we found the combination of collagen II and versican expression to be predictive, a relatively uncommon gene pair compared to the often studied

gene expression ratios of collagen II:I and aggrecan:versican. The selection appears reasonable, with one chondrocyte marker, collagen II, and one perichondrium marker, versican, used in the model and being inversely related to each other.

We showed how logistic regression can be used to estimate the histological score, a value bounded between 0 (worst) and 6 (best). Estimating GAG required modeling positive values only, therefore, we demonstrated how a generalized linear model with a gamma distribution and log-link could be implemented, similarly to other biomarker applications (García-Broncano et al., 2014; Schufreider et al., 2015). Stepwise selection was used again for the potency models, returning the combination of collagen II and MFAP5 for prediction of GAG, and MFAP5 alone for modeling histological MBS score. Increased MFAP5 expression

has been correlated with decreased chondrogenic potential in mesenchymal stem cells (Solchaga et al., 2010). MFAP-5 protein binds active TGF $\beta$ 1, TGF $\beta$ 2, and BMP2, sequestering these pro-chondrogenic factors in the matrix (Combs et al., 2013). Intracellular MFAP5 has been shown to bind and activate notch signaling (Miyamoto et al., 2006), which inhibits the regulator of cartilage formation, Sox9 (Hardingham et al., 2006). Notch has been found primarily in the perichondrium rather than the cartilage layer in mandibular condylar cartilage (Serrano et al., 2014), which, like nasal cartilage, is derived from cranial neural-crest cells (Chai et al., 2000). The predictive ability of these models are significant especially when considering that only ~30–40% of the variance in protein abundance is explained by mRNA levels (Vogel and Marcotte, 2012). The selection of different genes for each potency assay may be due to the fact that they assess quality in slightly different ways; the histological score includes information not only of the GAG content, but also about the morphology of the cells.

We observed that all pellets that contained at least 70% NC cells pass the clinical trial release criteria, i.e., histological score  $\geq 3$ , but more contamination could also lead to good results in some cases. To implement the purity assay, we propose a conservative three-category rating scale for the predicted purity (NC%), i.e., if cells are estimated to be more than 70% pure, they are labeled as *pure*, less than 50% pure, they are labeled as *fail*, otherwise the estimation is labeled as *uncertain*. We propose to introduce this uncertain region for the time being until further data can be collected and the estimates can be made more precise. In practice, we would recommend that starting cell populations labeled as pure or uncertain should continue in the production process, however, if the cells fail the purity test, the costly production should be halted. Cartilage engineered from cells of uncertain purity would nevertheless need to pass the release criteria (such as the histological score-based release criterion), ensuring the quality of the product.

The proposed models have been generated based on a limited number of genes. In future, it will be valuable to widen the panel of genes analyzed, based on other published studies (Dell'Accio et al., 2001) or more extensive unbiased transcriptomic analysis. The selected genes and coefficient estimates for the models will have to be updated as more data are obtained, and the in-process controls will have to be validated to meet GMP standards. Only then the models could be actually implemented as in-process control and release criteria, predicting if an engineered graft would pass or fail according to revised cut-off thresholds. Production would be stopped if the acceptance thresholds are not met. Moreover, the definition of a high quality graft may need to be revised as more long-term clinical outcome data are collected.

## CONCLUSION

In conclusion, we have put forward gene expression-based assays for identity, purity, and potency to help ensure the safe and effective clinical use of nasal chondrocyte-derived engineered cartilage. More generally, we provide an example of the development and implementation of purity and potency

assays based on relatively simple qPCR assays, stepwise selection of the most significant genes, and predictive *in silico* models. This approach could be relevant for the development of quality controls for other products in the emerging field of regenerative medicine, one of the biggest challenges for advanced therapy medicinal products to overcome for clinical translation.

## DATA AVAILABILITY STATEMENT

All datasets generated for this study are included in the article/**Supplementary Material**.

## ETHICS STATEMENT

Human nasal septum biopsies were collected from 17 donors (9 female, 8 male, mean age 46 years, range 16–84 years) after informed consent and in accordance with the local ethical commission (EKBB; Ref.# 78/07). Two samples derived from patients enrolled in the Nose2Knee clinical trials (ClinicalTrials.gov, numbers NCT01605201 and NCT02673905).

## AUTHOR CONTRIBUTIONS

MA conceived and designed the study. MA and LP performed the experiments, analyzed the data, and wrote the manuscript. LP created the models. AB contributed to the study design and revised the manuscript. MH and RK contributed to the sample preparation. DW contributed to manuscript revision. IM contributed to compiling the data and critically revised the manuscript.

## FUNDING

This project has received funding from the European Union's Seventh Program for Research, Technological Development and Demonstration under Grant Agreement No. 278807 (BIO-COMET) and the European Union's Horizon 2020 Research and Innovation Program under Grant Agreement No. 681103 (BIO-CHIP). This work was also supported by the Swiss National Science Foundation as part of the NCCR Molecular Systems Engineering (Project Number 51NF40-141825).

## ACKNOWLEDGMENTS

We would like to thank Sandra Feliciano for her help with sample analysis. Thanks to Dr. Florian Geier and Dr. Julien Roux for the statistical analysis discussions. Thanks also to Dr. Sylvie Miot and Anke Wixmerten for critically reading the manuscript.

## SUPPLEMENTARY MATERIAL

The Supplementary Material for this article can be found online at: <https://www.frontiersin.org/articles/10.3389/fbioe.2020.00283/full#supplementary-material>

## REFERENCES

- Agostini, M., Zangrando, A., Pastrello, C., D'Angelo, E., Romano, G., Giovannoni, R., et al. (2015). A functional biological network centered on XRCC3: a new possible marker of chemoradiotherapy resistance in rectal cancer patients. *Cancer Biol. Ther.* 16, 1160–1171. doi: 10.1080/15384047.2015.1046652
- Aksoy, F., Yildirim, Y., Demirhan, H., Özturan, O., and Solakoglu, S. (2012). Structural characteristics of septal cartilage and mucoperichondrium. *J. Laryngol. Otol.* 126, 38–42. doi: 10.1017/S0022215111002404
- Al Dayeh, A., and Herring, S. (2014). Compressive and tensile mechanical properties of the porcine nasal septum. *J. Biomech.* 47, 154–161.
- Asnaghi, M. A., Dühr, R., Quasnicka, H., Hollander, A., Kafienah, W., Martin, I., et al. (2018). Chondrogenic differentiation of human chondrocytes cultured in the absence of ascorbic acid. *J. Tissue Eng. Regen. Med.* 12, 1402–1411. doi: 10.1002/term.2671
- Bairati, A., Comazzi, M., and Gioria, M. (1996). A comparative study of perichondrial tissue in mammalian cartilages. *Tissue Cell* 28, 455–468.
- Baker, J., and Caterson, B. (1978). The isolation of "link proteins" from bovine nasal cartilage. *Biochim. Biophys. Acta* 532, 249–258.
- Barbosa, I., Garcia, S., Barbier-Chassefière, V., Caruelle, J. P., Martelly, I., and Papy-García, D. (2003). Improved and simple micro assay for sulfated glycosaminoglycans quantification in biological extracts and its use in skin and muscle tissue studies. *Glycobiology* 13, 647–653.
- Bravery, C., Carmen, J., Fong, T., Oprea, W., Hoogendoorn, K., Woda, J., et al. (2013). Potency assay development for cellular therapy products: an ISCT review of the requirements and experiences in the industry. *Cytotherapy* 15, 9–19. doi: 10.1016/j.jcyt.2012.10.008
- Buckwalter, J., and Mankin, H. (1998). Articular cartilage repair and transplantation. *Arthritis Rheum.* 41, 1331–1342.
- Carmen, J., Burger, S. R., McCaman, M., and Rowley, J. A. (2012). Developing assays to address identity, potency, purity and safety: cell characterization in cell therapy process development. *Regen. Med.* 7, 85–100. doi: 10.2217/rme.11.105
- Chai, Y., Jiang, X., Ito, Y., Bringas, P., Han, J., Rowitch, D., et al. (2000). Fate of the mammalian cranial neural crest during tooth and mandibular morphogenesis. *Development* 127, 1671–1679.
- Combs, M., Knutsen, R., Broekelmann, T., Toennies, H., Brett, T., Miller, C., et al. (2013). Microfibril-associated glycoprotein 2 (MAGP2) loss of function has pleiotropic effects in vivo. *J. Biol. Chem.* 288, 28869–28880. doi: 10.1074/jbc.M113.497727
- Committee for Medicinal Products for Human Use [CHMP] (2008). *EMA/CHMP/410869/2006: Guideline on Human Cell-Based Medicinal Products*. Amsterdam: European Medicines Agency.
- Committee for Medicinal Products for Human Use [CHMP] (2017). *CHMP Assessment Report, Spherox, Procedure No. EMA/H/C/002736/0000*. Amsterdam: European Medicines Agency.
- Dell'Accio, F., De Bari, C., and Luyten, F. (2001). Molecular markers predictive of the capacity of expanded human articular chondrocytes to form stable cartilage in vivo. *Arthritis Rheum.* 44, 1608–1619.
- Detela, G., and Lodge, A. (2019). EU regulatory pathways for ATMPs: standard, accelerated and adaptive pathways to marketing authorisation. *Mol. Ther. Methods Clin. Dev.* 13, 205–232. doi: 10.1016/j.omtm.2019.01.010
- Diaz-Romero, J., Kürsener, S., Kohl, S., and Nescic, D. (2017). S100B + A1 CELISA: a novel potency assay and screening tool for redifferentiation stimuli of human articular chondrocytes. *J. Cell. Physiol.* 232, 1559–1570.
- Editorial (2009). Identity crisis. *Nature* 457, 935–936.
- Faraway, J. (2006). *Extending the Linear Model with R: Generalized Linear, Mixed Effects and Nonparametric Regression Models*. Boca Raton, FL: Chapman & Hall.
- García-Broncano, P., Berenguer, J., Fernández-Rodríguez, A., Pineda-Tenor, D., Jiménez-Sousa, M., García-Alvarez, M., et al. (2014). PPAR $\gamma$ 2 Pro12Ala polymorphism was associated with favorable cardiometabolic risk profile in HIV/HCV coinfecting patients: a cross-sectional study. *J. Transl. Med.* 12:235.
- Grogan, S., Barbero, A., Winkelmann, V., Rieser, F., Fitzsimmons, J., O'Driscoll, S., et al. (2006). Visual histological grading system for the evaluation of in vitro-generated neocartilage. *Tissue Eng.* 12, 2141–2149.
- Halper, J., and Kjaer, M. (2014). Basic components of connective tissues and extracellular matrix: elastin, fibrillin, fibulins, fibrinogen, fibronectin, laminin, tenascins and thrombospondins. *Adv. Exp. Med. Biol.* 802, 31–47. doi: 10.1007/978-94-007-7893-1\_3
- Hardin, J., and Hilbe, J. (2007). *Generalized Linear Models and Extensions*. College Station, TX: Stata Press.
- Hardingham, T., Oldershaw, R., and Tew, S. (2006). Cartilage, SOX9 and Notch signals in chondrogenesis. *J. Anat.* 209, 469–480.
- Hellingman, C., Verwiël, E., Slagt, I., Koevoet, W., Poulton, R., Nolst-Trenité, G., et al. (2011). Differences in cartilage-forming capacity of expanded human chondrocytes from ear and nose and their gene expression profiles. *Cell Transplant.* 20, 925–940. doi: 10.3727/096368910X539119
- Hosmer, D., Lemeshow, S., and Sturdivant, R. (2013). *Applied Logistic Regression*, 3rd Edn. Hoboken, NJ: Wiley.
- Hothorn, T., Bretz, F., and Westfall, P. (2008). Simultaneous inference in general parametric models. *Biom. J.* 50, 346–363. doi: 10.1002/bimj.200810425
- Hyun-woo, N. (2019). *Kolon's Stance on Invozza Draws Backlash*. Los Angeles, CA: The Korea Times.
- Jackman, S. (2017). *pscl: Classes and Methods for R Developed in the Political Science Computational Laboratory*. Sydney: United States Studies Centre.
- Jakob, M., Démarteau, O., Schäfer, D., Stumm, M., Heberer, M., and Martin I. (2003). Enzymatic digestion of adult human articular cartilage yields a small fraction of the total available cells. *Connect. Tissue Res.* 44, 173–180. doi: 10.1080/03008200390215836
- Kon, E., Gobbi, A., Filardo, G., Delcogliano, M., Zaffagnini, S., and Marcacci, M. (2009). Arthroscopic second-generation autologous chondrocyte implantation compared with microfracture for chondral lesions of the knee: prospective nonrandomized study at 5 years. *Am. J. Sports Med.* 37, 33–41. doi: 10.1177/0363546508323256
- Lehoczky, G., Wolf, F., Mumme, M., Gehmert, S., Miot, S., Haug, M., et al. (2019). Intra-individual comparison of human nasal chondrocytes and debrided knee chondrocytes: relevance for engineering autologous cartilage grafts. *Clin. Hemorheol. Microcirc.* 74, 67–78. doi: 10.3233/CH-199236
- Lele, S., Keim, J., and Solymos, P. (2019). *ResourceSelection: Resource Selection (Probability) Functions for Use-Availability Data. R package version 0.2-4*.
- Liu, S., Lu, M., Li, H., and Zuo, Y. (2019). Prediction of gene expression patterns with generalized linear regression model. *Front. Genet.* 10:120. doi: 10.3389/fgene.2019.00120
- Maertzdorf, J., McEwen, G., Weiner, J., Tian, S., Lader, E., Schriek, U., et al. (2016). Concise gene signature for point-of-care classification of tuberculosis. *EMBO Mol. Med.* 8, 86–95. doi: 10.15252/emmm.201505790
- Martin, I., Jakob, M., Schäfer, D., Dick, W., Spagnoli, G., and Heberer, M. (2001). Quantitative analysis of gene expression in human articular cartilage from normal and osteoarthritic joints. *Osteoarthritis Cartilage* 9, 112–118.
- Miyamoto, A., Lau, R., Hein, P., Shipley, J., and Weinmaster, G. (2006). Microfibrillar proteins MAGP-1 and MAGP-2 induce Notch1 extracellular domain dissociation and receptor activation. *J. Biol. Chem.* 281, 10089–10097.
- Mollenhauer, J., and Gaissmaier, C. (2010). Methods of determining chondrocytes. U. S. Patent No 9,080,213. Washington, DC: U.S. Patent and Trademark Office.
- Mumme, M., Barbero, A., Miot, S., Wixmertens, A., Feliciano, S., Wolf, F., et al. (2016). Nasal chondrocyte-based engineered autologous cartilage tissue for repair of articular cartilage defects: an observational first-in-human trial. *Lancet* 388, 1985–1994. doi: 10.1016/S0140-6736(16)31658-0
- Ono, N., Ono, W., Mizoguchi, T., Nagasawa, T., Frenette, P., and Kronenberg, H. (2014). Vasculature-associated cells expressing nestin in developing bones encompass early cells in the osteoblast and endothelial lineage. *Dev. Cell* 29, 330–339. doi: 10.1016/j.devcel.2014.03.014
- Popko, M., Bleys, R., De Groot, J., and Huizinga, E. (2007). Histological structure of the nasal cartilages and their perichondrial envelope. I. The septal and lobular cartilage. *Rhinology* 45, 148–152.
- R Core Team (2019). *R: A Language and Environment for Statistical Computing*. Vienna: R Foundation for Statistical Computing. Available online at: <http://www.r-project.org/index.html>
- Rapko, S., Zhang, M., Richards, B., Hutto, E., Dethlefsen, S., and Duguay, S. (2010). Identification of the chondrocyte lineage using microfibril-associated glycoprotein-2, a novel marker that distinguishes chondrocytes from synovial cells. *Tissue Eng. Part C* 16, 1367–1375. doi: 10.1089/ten.TEC.2009.0772
- Schuffreider, A., McQueen, D., Lee, S., Allon, R., Uhler, M., Davie, J., et al. (2015). Diminished ovarian reserve is not observed in infertility patients with high

- normal CGG repeats on the fragile X mental retardation 1 (FMR1) gene. *Hum. Reprod.* 30, 2686–2692.
- Scotti, C., Tonnarelli, B., Papadimitropoulos, A., Scherberich, A., Schaeren, S., Schauerte, A., et al. (2010). Recapitulation of endochondral bone formation using human adult mesenchymal stem cells as a paradigm for developmental engineering. *Proc. Natl. Acad. Sci. U.S.A.* 107, 7251–7256. doi: 10.1073/pnas.1000302107
- Serrano, M., So, S., and Hinton, R. (2014). Roles of notch signalling in mandibular condylar cartilage. *Arch. Oral Biol.* 59, 735–740. doi: 10.1016/j.archoralbio.2014.04.003
- Shibata, S., Fukada, K., Suzuki, S., Ogawa, T., and Yamashita, Y. (2001). Histochemical localisation of versican, aggrecan and hyaluronan in the developing condylar cartilage of the fetal rat mandible. *J. Anat.* 198, 129–135.
- Solchaga, L., Penick, K., Goldberg, V., Caplan, A., and Welter, J. (2010). Fibroblast growth factor-2 enhances proliferation and delays loss of chondrogenic potential in human adult bone-marrow-derived mesenchymal stem cells. *Tissue Eng. Part A* 16, 1009–1019. doi: 10.1089/ten.TEA.2009.0100
- Späth, S., Andrade, A., Chau, M., Baroncelli, M., and Nilsson, O. (2018). Evidence that rat chondrocytes can differentiate into perichondrial cells. *JBMR Plus* 2, 351–361. doi: 10.1002/jbm4.10056
- Spicer, A. P., Joo, A., and Bowling, R. A. (2003). A hyaluronan binding link protein gene family whose members are physically linked adjacent to chondroitin sulfate proteoglycan core protein genes: the missing links. *J. Biol. Chem.* 278, 21083–21091.
- Tay, A., Farhadi, J., Suetterlin, R., Pierer, G., Heberer, M., and Martin, I. (2004). Cell yield, proliferation, and postexpansion differentiation capacity of human ear, nasal, and rib chondrocytes. *Tissue Eng.* 10, 762–770.
- Tekari, A., Luginbuehl, R., Hofstetter, W., and Egli, R. (2014). Chondrocytes expressing intracellular collagen type II enter the cell cycle and co-express collagen type I in monolayer culture. *J. Orthop. Res.* 32, 1503–1511. doi: 10.1002/jor.22690
- Teo, A. Q. A., Wong, K. L., Shen, L., Lim, J. Y., Toh, W. S., Lee, E. H., et al. (2019). Equivalent 10-year outcomes after implantation of autologous bone marrow-derived mesenchymal stem cells versus autologous chondrocyte implantation for chondral defects of the knee. *Am. J. Sports Med.* 47, 2881–2887. doi: 10.1177/0363546519867933
- Thej, C., and Kumar Gupta, P. (2019). *The Role of Mesenchymal Stromal Cells in the Management of Osteoarthritis of the Knee*. London: IntechOpen.
- Upton, J., and Glowacki, J. (1981). Neocartilage derived from transplanted perichondrium: what is it? *Plast. Reconstr. Surg.* 68, 166–172.
- Van Osch, G., Van Der Veen, S., Burger, E., and Verwoerd-Verhoef, H. (2000). Chondrogenic potential of in vitro multiplied rabbit perichondrium cells cultured in alginate beads in defined medium. *Tissue Eng.* 6, 321–330.
- Vogel, C., and Marcotte, E. (2012). Insights into the regulation of protein abundance from proteomic and transcriptomic analyses. *Nat. Rev. Genet.* 13, 227–232. doi: 10.1038/nrg3185
- Wei, T., and Simko, V. (2017). *R Package “Corrplot”: Visualization of a Correlation Matrix. R package version 0.84.*
- Ying, J., Wang, Q., Xu, T., and Lyu, J. (2018). Establishment of a nine-gene prognostic model for predicting overall survival of patients with endometrial carcinoma. *Cancer Med.* 7, 2601–2611. doi: 10.1002/cam4.1498
- Zhao, L., Chen, Y., and Schaffner, D. (2001). Comparison of logistic regression and linear regression in modeling percentage data. *Appl. Environ. Microbiol.* 67, 2129–2135.

**Conflict of Interest:** The authors declare that the research was conducted in the absence of any commercial or financial relationships that could be construed as a potential conflict of interest.

Copyright © 2020 Asnaghi, Power, Barbero, Haug, Köppl, Wendt and Martin. This is an open-access article distributed under the terms of the Creative Commons Attribution License (CC BY). The use, distribution or reproduction in other forums is permitted, provided the original author(s) and the copyright owner(s) are credited and that the original publication in this journal is cited, in accordance with accepted academic practice. No use, distribution or reproduction is permitted which does not comply with these terms.